Accessibility and Trajectory Planning of Cutter Changing Robot Arm for Large-Diameter Slurry Shield

Mei YANG*, Guiying ZENG**, Yong REN***, Laikuang LIN****, Wei KE*****,
Yifan LIU******

*College of Mechanical and Electrical Engineering, State Key Laboratory of High Performance Complex Manufacturing, Central South University, China, E-mail: 183701027@csu.edu.cn
**College of Mechanical and Electrical Engineering, State Key Laboratory of High Performance Complex Manufacturing, Central South University, China, E-mail: jdszgy@163.com
***China Railway Construction Heavy Industry Co. Ltd., China, E-mail: renyonghi@126.com
****College of Mechanical and Electrical Engineering, State Key Laboratory of High Performance Complex Manufacturing, Central South University, China, E-mail: linlaikuang@csu.edu.cn (Corresponding author)
*****China Railway Construction Heavy Industry Co. Ltd., China, E-mail: 919663928@qq.com
******College of Mechanical and Electrical Engineering, State Key Laboratory of High Performance Complex Manufacturing, Central South University, China, E-mail: 1070516037@qq.com

1. Introduction

For long-distance tunnels, shield tunneling is the preferred construction method, and has been widely used in municipal, railway, highway projects, and shield machine has become the major technical equipment for national infrastructure construction, resource exploitation and defense construction [1-4]. As the core part of shield machine, the cutter directly cuts the rock and soil on the excavation face, which inevitably leads to serious wear and fracture failure in the tunneling process. If it is not replaced in time, the tunneling efficiency will be greatly reduced. Therefore, it is necessary to stop the machine and open the chamber to check and replace the worn cutter in time during shield tunnel construction [5-7]. For cutter-changing operation, manual work is the main procedure as shown in Fig. 1. It requires professional worker enter the excavation chamber frequently to complete difficult cutter-changing assignments, which not only cause high cost and long time, restricting the construction efficiency, but also has great security risk for worker in high pressure and humidity environment, even causing casualties [8-10]. Therefore, it is urgent to design a cutter changing robot to realize the safe and efficient operation in high-risk environment. However, the internal space of the shield machine is narrow and complex, and the layout of cutters to be re-placed on the cutterhead is wide and complex, which makes it difficult to design the configuration, size and the trajectory planning of the robot arm, and has great challenge to plan the cutter-changing trajectory of robot arm.

Fig. 1 Manual cutter changing process

A lot of research on cutter change robot technology has been carried out by relevant institutions. French Bouy-gues group has designed a 'TELEMECH' type tool changing robot, including KUKA arm and specific manipulator, and the operation experiment has been carried out in a Hong Kong tunnel project, only 30% of cutters on the cutterhead can be replaced [11]. German artificial intelligence research and development center has developed a 5-DOF hydraulic cutter changing robot with compact structure, covering 75% of cutters [12]. Domestic research on cutter change robot is still in the early phase. Huo proposed a cutter holder suitable for cutter changing robot, which can realize quick disassembly and assembly of cutter [13]. Xia completed configuration design and dimension synthesis of cutter disassembly mechanism for cutter change robot based on performance atlas [14]. Yang proposed a trajectory planning method of cutter change robot based on binocular vision and visual navigation technology [15]. However, the above research on the cutter change robot of shield machine mainly focuses on the design of manipulator and cutter holder system, and is in the stage of design and experiment. There are few researches about the cutter change robot arm.

Cutter changing robot belongs to jointed serial robot. scholars have studied the cutter change trajectory planning based on forward and inverse kinematics analysis, where forward kinematics is applied to determine the joint positions and get the gesture and position of the actuator, and inverse kinematics refers to how to determine the corresponding joint positions when the robot reaches the expected position [16-18]. Xie designed an 8-DOF tunnel shotcrete manipulator, introducing virtual joint and DH method to establish the kinematics model of the robot, and carried out the optimal spraying trajectory planning [19]. Wang proposed an accurate inverse kinematics algorithm combining analytical method and numerical method, which was successfully applied to a 7-DOF spraying robot [20]. Based on a six-leg mechanism with one degree of freedom, Zhang proposed a comprehensive calculation method of configuration and dimension, where the feasible length range of the connecting rod can be obtained quickly [21]. Liu put forward an autonomous obstacle avoidance trajectory planning method using dangerous scene information based on the kinematic model of space robot [22]. Zhang [23] and Fung [24] respectively completed the optimal path

planning of wood repair robot and glass handling robot based on the minimum time and energy. Li [25] designed an optimal measurement pose number searching method for kinematic calibration of six-DOF serial robot. Xu put forward a regional directional acquisition method based on two-arm cooperation, which was successfully applied to the target trajectory planning of astronautic manipulator [26]. Augustaitis [27] used geometric methods to solve the robot inverse kinematics and proposed a theoretical approach to solve the inverse kinematics solution using the global projection of the robot linkage. The above research shows that the forward kinematics modelling, the inverse kinematics solving and the trajectory planning of different target pose are the basis for the structural design of the robot arm.

Considering the cutter changing requirements and narrow space constraints of the shield machine, the configuration of the cutter change robot arm is designed. Taking the working section and the length of the manipulator as the objective function, the length parameters of the robot arm is designed. The forward kinematics model of the robot arm is established to check it's the reachable workspace in shield machine. Based on the inverse kinematics solution of the manipulator, the trajectory planning of all cutters on one auxiliary arm of the cutterhead is completed, the motion performance of the robot arm is analyzed by ADAMS software. Finally, the test platform of the cutter change robot is built, and the feasibility of the configuration and size design of the cutter change robot is verified.

2. Configuration of cutter changing robot arm

The cutter changing robot is intended for automatically dismounting the worn cutter from cutterhead and installing the new cutter during TBM construction. The cutter changing robot is arranged in the storage cabin, which is fixed at the behind cabin. The cutter changing robot is contracted in the storage room with door closed during TBM regular excavation. While the cutter changing robot is required to move out of the cabin and reach the behind of cutterhead to change the worn cutter during downtime maintenance period.

Taking an existing shield machine with 8.8m diameter as the design object, the configuration of the cutter changing robot is designed according to the inner spatial characteristics and limitation of the cutterhead. In order to reduce the change of shield machine overall design scheme as far as possible, it is considered that the human cabin is designed as the storage cabin of the cutter changing robot with the dimension of 1150×1180×3090 mm, which restricts the overall size of the cutter changing robot.

The cutter is arranged on the radial spoke of the cutterhead in the shape of "meter", before the cutter changing operation, the cutterhead can rotate to the position, where the cutter to be changed is near to the storage cabin [28-29]. It can reduce the motion range requirement of robot arm. Therefore, the robot arm is designed to reach the position of all cutters on a certain radial spoke, as Fig. 2, a shown. Taking the storage cabin and cutter on the spoke arm as starting point and ending point, respectively, the main extension area of the robot arm is in the mud water balance chamber with 8630 mm diameter and 995 mm depth, the air cushion chamber with 8630 mm diameter and 1425 mm depth, and four tilted brackets arranging at the back of cut-

terhead, as shown in Fig. 2, b [30]. The robot arm is designed with six degrees of freedom, which can effectively avoid the collision with the inner structure of shield machine.
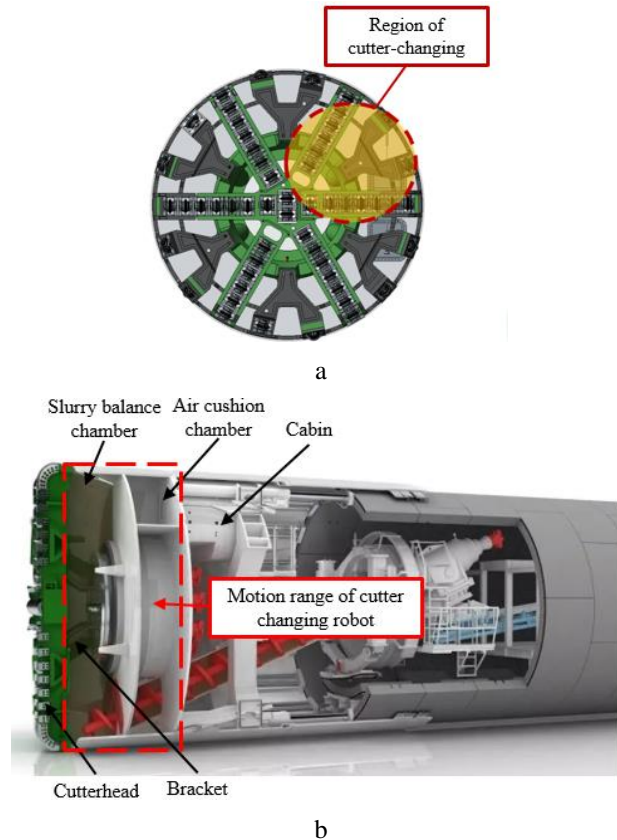

a

b

Fig. 2 Workspace analysis of cutter changing robot: a) region of cutter-changing; b) motion range of cutter changing robot

The main function of the robot arm is to carry the end manipulator and cutter, and transport them between storage cabin and cutter housing on the cutterhead, and the robot is determined as jointed serial. During tunneling condition of shield machine, the cutter change robot should contract in the storage cabin. While in the condition of cutter changing operation, the gate of cabin is opened to let the cutter change robot extend out to work. Therefore, the robot arm needs one or more horizontal prismatic joint, which can realize by sliding mechanism or telescope joints. As the cutter holder is welded on the cutterhead, which means the manipulator should complete the disassembly and assembly operation at the vertical direction. It requires the robot arm has at least four links and four degrees of freedom, including three rotational degrees of freedom and one translational degree of freedom. Four kinds of manipulator configuration schemes are designed, as shown in Fig. 3.

Due to the heavy weight of the whole robot, the sliding rail type is adopted for the mobile joint of robot base. The base and guide rail of the robot are set on the top of the storage cabin.

In scheme 1, the motion of the first rotary joint is limited by the storage chamber, as the slide way should arranged in the storage cabin. While in scheme 2, the telescopic joint is close to the base, seriously restricting its flexibility when replacing the cutter in non-horizontal position. The second movable joint of scheme 3 is arranged inside the

storage cabin and its size is directly limited by the size of storage cabin. Scheme 4 includes one mobile joint, three rotary joints and one telescopic joint with a large range of cutter-changing and flexible movement. It meets the expected

requirements of freedom degree and convenience, and is more suitable for cutter change operation in narrow shield machine.
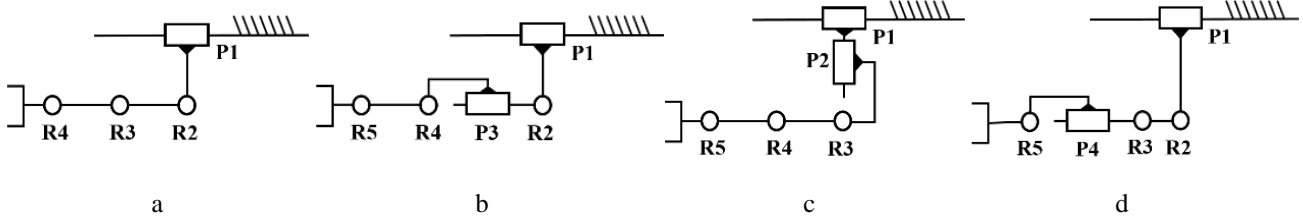

Fig. 3 Kinematic diagrams of cutter changing robot arm: a) scheme 1; b) scheme 2; c) scheme 3; d) scheme 4

In the actual cutter change procedure, the cutterhead is difficult to stop precisely at the present position of the robot. As shown in Fig. 4, OA is the desired position of the radial spoke, and A_1 is the desired position of cutter to be replaced, while OB and B_1 are the corresponding actual positions. The angle error of radial spoke is set as β, the angle error of cutter is β, and the displacement error of cutter is defined as α. Two rotary joints are added at both ends of the robot arm to make it rotate in the direction perpendicular to the cutterhead axis, so as to compensate the angle of the end manipulator. In addition, a translational degree of freedom is added to the end manipulator to compensate error displacement of cutter. The final configuration of the robot arm is shown in Fig. 5.
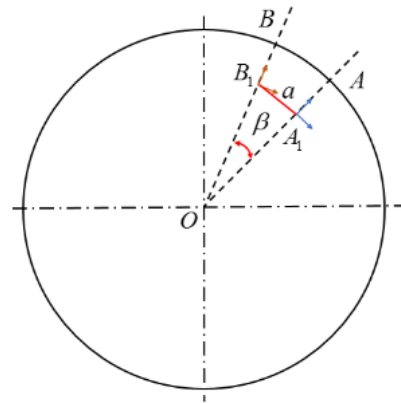
The design scheme of the manipulator of the robot is shown in Fig. 6, including the base moving joint, the rotating joint, the pitching joint of big arm, the pitching joint of forearm, stretchable joint of forearm and the end pitching joint. Because the cutter change robot needs to bear large load, the hydraulic driving is used to achieve high energy density. During the cutter change operation, the end manipulator assembles the cutter into the housing, disassembles the cutter out of the housing.
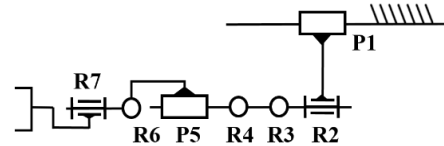

Fig. 4 The actual position of cutterhead and cutter

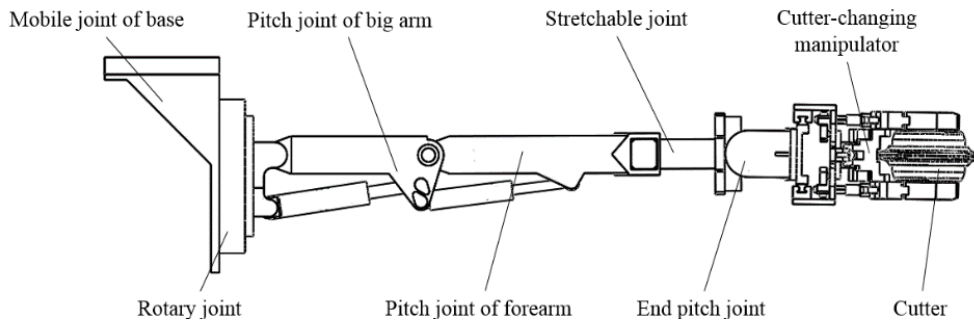Fig. 5 Final kinematic diagrams of cutter changing robot arm

Fig. 6 Configuration model of cutter changing robot

3. Dimension design of cutter changing robot arm

To determine the length of each link and the motion range of each moving pair for the robot arm, the structure design and calculation are carried out based on the end posture and workspace of the robot arm, where the workspace and the total length of the manipulator are important factors to be considered and the overall size and mass should be as small as possible.

3.1. Optimization model of cutter changing robot arm

1) Design variable of cutter changing robot arm. The structural diagram of the robot arm is shown in Fig. 7.

Joint 1 is the moving joint of the base and joint 2 is the rotation joint of the arm, which have no effect on the workspace section size of the arm. Therefore, these two parameters are not selected as design variables. Set the angle of joint 3 as θ_1, the length of big arm as L_2, and the angle of joint 4 as θ_2. The joint 5 is expansion joint, in addition, set the length of outer arm of telescopic arm as L_3, and set the longest stretch of inner arm as L_4, the total length of telescopic arm as L'_3, the angle of joint 6 as θ_3, and the length of joint 6 to end translation mechanism as L_5. Therefore, the design variables of the robot arm can be obtained as,

$$X = [L_2, L'_3, L_5, \theta_1, \theta_2, \theta_3] = [x_1, x_2, x_3, x_4, x_5, x_6].$$
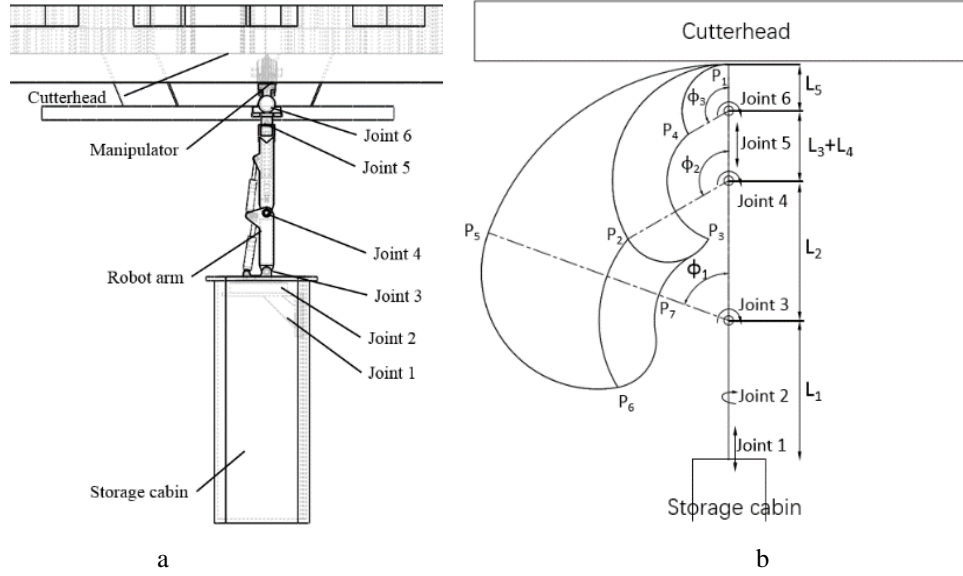
Fig. 7 Structure and working section of manipulator: a) actual model of robot arm; b) simplified model of robot arm

2) Objective function and constraints. On the premise that the robot arm can reach the positions of all cutters on the cutter head, the working section of the robot arm should be as small as possible. Therefore, the area of the working section of the robot arm is taken as the objective function. As shown in Fig. 7, b, the working section of the robot arm mainly includes three arc-shaped areas: $P_1P_2P_3P_4$ at the end of the arm, $P_1P_5P_6P_2$ swept by the circular arc P_1P_2 and the area $P_2P_6P_7P_3$ swept by the circular arc 0, their areas S_1, S_2, S_3 can be calculated respectively.

$$\begin{cases} S_1 = \left|\varphi_2(1-\cos\varphi_3)\right|L_3'(L_5+675) \\ S_2 = \left|\varphi_1(1-\cos\varphi_2)\right|L_2(L_3'+L_5+675) \\ S_3 = \left|\varphi_1\left\{L_3'(1-\cos\varphi_3+L_2[\cos\varphi_2-\cos(\varphi_2+\varphi_3)]\right\}\right|(L_5+675) \end{cases}, . \quad (1)$$

where: φ_i is the limit rotation angle of the ith connection rod, $\theta_{imin} = \pi - \varphi_i$, and $\varphi_i > 0$.

The total area of the workspace section for the robot arm is:

$$S = S_1 + S_2 + S_3 = \left|\varphi_2(1-\cos\varphi_3)\right|L_3'L_5 + \left|\varphi_1(1-\cos\varphi_2)\right|L_2(L_3'+L_5) + \left|\varphi_1\left\{L_3'(1-\cos\varphi_3+L_2[\cos\varphi_2-\cos(\varphi_2+\varphi_3)]\right\}\right|L_5. \quad (2)$$

The objective function 1 about the total area of workspace section is built:

$$minF_1(X) = (\pi-x_2)(1+\cos x_6)x_2x_3 + (\pi-x_4)(1+\cos x_5)x_1(x_2+x_3) + \\ + (\pi-x_4)\left\{x_2(1+\cos x_6) - x_1[\cos x_5 + \cos(x_5+x_6)]\right\}x_3. \quad (3)$$

In order to get a small size and light weight robot arm, the sum of the length of the robot arm should be as short as possible, which is taken as the objective function 2:

$$minF_2(X) = x_1 + x_2 + x_3. \quad (4)$$

The above two objective functions are integrated into a comprehensive objective function:

$$minF(X) = k_1F_1(X) + k_2F_2(X), \quad (5)$$

where: k_i is the weight of the ith objective function, which means the importance degree. In the process of cutter changing, the total length of the robot arm and the workspace areas are of equal importance, therefore, the weight allocation set of the objective function can be set as $k_1 = k_2 = 0.5$.

In order to ensure that the arm can reach all the cutters on the cutterhead, the farthest distance between the working section and the arm should be larger than the radius of the cutterhead.

$$x_1\sin x_4 + x_2 + x_3 \geq 4400. \quad (6)$$

According to the specific structure of the robot arm, corresponding constraints of the joints are built:

$$\begin{cases} 1.784 \leq x_4 \leq \pi \\ 1.308 \leq x_5 \leq \pi . \\ 0 \leq x_6 \leq \pi \end{cases} \quad (7)$$

3) Optimization of cutter changing robot arm. Genetic algorithm is used to optimize the objective function by Matlab software, and the results are obtained.

$$X = [732.26, 1953.21, 433.92, 2.339, 1.6258, 0.017]. \quad (8)$$

To facilitate machining, the results are rounded as: L_2=732 mm, L_3'=1960 mm, L_5=435 mm, θ_1=134°, θ_2=95°, θ_3=0°. In order to increase the motion range of the joint, the angle ranges of joint 3 and joint 4 are taken as 134-195° and 95-205°, respectively. For joint 5, L_3' is total length of telescopic arm with telescopic range is 1310-1960 mm, where

the length of the outer arm and the inner arm is 1100 mm and 860 mm respectively. Joint 6 is a swing joint, and the swing range is 0-3000 mm. Joint 2 is a rotary joint, and the rotation range is 0-360°, intending to replace all cutters on the cutterhead.

During the shield tunneling, the manipulator shrinks into the storage cabin with the dimension of 1150×1180×3090 mm, as shown in Fig. 8.
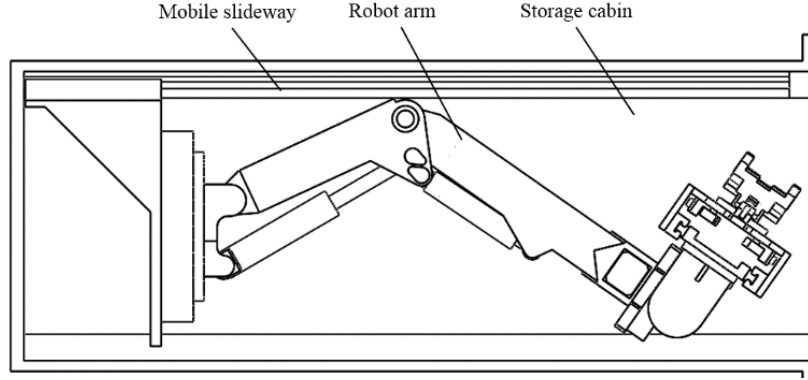

Fig. 8 Contracted state of cutter changing robot in storage cabin

3.2. Reachable domain of cutter changing robot arm

1) Kinematic model of cutter changing robot arm. The robot arm is connected by multiple links through motion pairs. The coordinate system is established at the center of each joint, and the position and posture of each joint coordinate system in Cartesian coordinate system are obtained through corresponding coordinate transformation. In this study, the improved Denavit-Hartenberg method is used to build the kinematic model of the joint, and the transformation relationship between each coordinate system of the arm is established through homogeneous transformation.
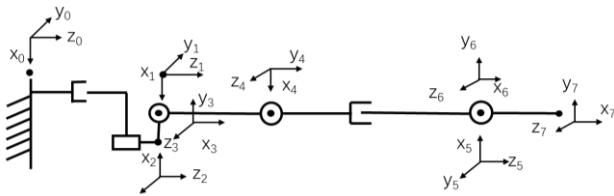

Fig. 9 D-H simplified model of cutter changing robot arm

Then, the relationship between the position of the

end cutter centroid of the robot arm in the Cartesian coordinate system and the joint coordinate system can be obtained. The D-H coordinate system is shown in Fig. 9, and the D-H parameters are shown in Table 1.

Table 1

D-H parameter table of the cutter change robot arm

Coordinate i	θ_i	d_i	a_{i-1}	α_{i-1}	Variable scope
1	0	d_1	0	0	0~3000mm
2	θ_2	0	560	0	0~360°
3	θ_3	0	100	-90°	-125~-75°
4	θ_4	0	732	0	-150~-65°
5	180°	d_5	0	-90°	1420~2070 mm
6	θ_6	0	0	-90°	-180~0°
7	0	0	460	0	/

Based on the rigid body kinematics translation and rotation theory, the base coordinate system and cutter centroid coordinate system is connected through 4×4 homogeneous transformation matrix，and the transformation matrix $_{i-1}^{i}T$ of adjacent coordinate system is as following:

$$_{i-1}^{i}T = \begin{bmatrix} cos\theta_i & -sin\theta_i & 0 & a_{i-1} \\ sin\theta_i cos\alpha_{i-1} & cos\theta_i cos\alpha_{i-1} & -sin\alpha_{i-1} & -sin\alpha_{i-1}d_i \\ sin\theta_i sin\alpha_{i-1} & sin\alpha_{i-1} & cos\alpha_{i-1} & cos\alpha_{i-1}d_i \\ 0 & 0 & 0 & 1 \end{bmatrix}, \quad (9)$$

$$_{0}^{i}T = {}_{0}^{1}T \cdot {}_{1}^{2}T \cdot \cdots {}_{i-1}^{i}T. \quad (10)$$

The space pose of the end cutter centroid of the robot arm can be obtained from Eq. (9) and (10) as following:

$$_{0}^{7}T = {}_{0}^{1}T {}_{1}^{2}T {}_{2}^{3}T {}_{3}^{4}T {}_{4}^{5}T {}_{5}^{6}T {}_{6}^{7}T = \begin{bmatrix} R & P \\ 0 & 1 \end{bmatrix} = \begin{bmatrix} n_x & o_x & a_x & p_x \\ n_y & o_y & a_y & p_y \\ n_z & o_z & a_z & p_z \\ 0 & 0 & 0 & 1 \end{bmatrix}, \quad (11)$$

$$n_x = -S_{346}C_2,$$
$$n_y = -S_{346}S_2,$$
$$n_x = -C_{346},$$
$$o_x = C_{346}C_2C_7 - S_2S_{27},$$
$$o_y = C_2S_7 + C_{346}C_7S_2,$$
$$o_z = -S_{346}C_7,$$
$$a_x = C_7S_2 + C_{346}C_2C_7,$$
$$a_y = C_{346}S_2S_7 - C_2C_7,$$
$$a_z = -C_{346}S_7,$$
$$p_x = 100C_2 + 732C_2C_3 - d_5\left(C_2C_3S_4 + C_2S_3C_4\right) + 460C_6\left(C_2S_3S_4 - C_2C_3C_4\right) + 460S_6\left(C_2C_3S_4 - C_2S_3C_4\right) - d_7S_2 + 560,$$
$$p_y = 100S_2 + 732C_3S_2 + d_7C_2 - d_5S_2S_{34} - 460S_2C_{34}C_6 + 460S_2S_{34}S_6,$$
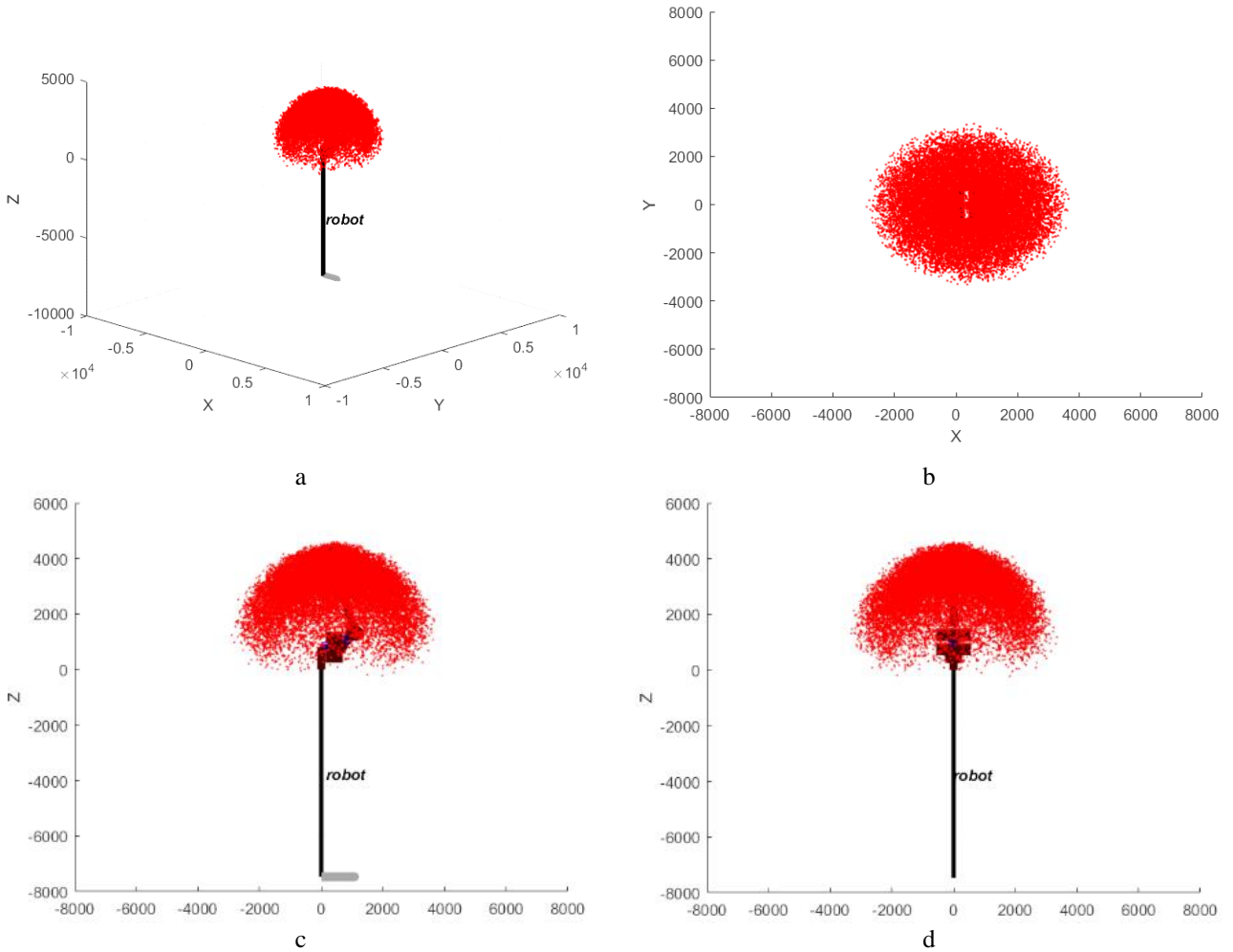$$p_z = d_1 + 460S_{346} - 732S_3 - d_5C_{34}. \tag{12}$$

Fig. 10 Working space of cutter changing robot: a) workspace of robot arm; b) workspace in XOY plane; c) workspace in XOZ plane; d) workspace in YOZ plane

where: $R = [n, o, a]$ is posture matrix of end coordinate system, and n, o, a are direction cosines of the three coordinate axes, respectively. $P = [P_x, P_y, P_z]$ is the position matrix of end coordinate system, and P_x, P_y, P_z are the origin coordinates of the end coordinate system. The numerical results are as follows, where: $S_i = sin(\theta_i)$, $C_i = cos(\theta_i)$, $S_{ij} = sin(\theta_i + \theta_j)$, $C_{ij} = cos(\theta_i + \theta_j)$.

The position vector of cutter centroid is a function about θ and d. When the angles θ_i of joints 2, 3, 4 and 6 and the lengths d_i of joints 1 and 5 are known, the pose vector n, o, a, p can be calculated, and the pose of the cutter centroid relative to the base coordinate system can be determined.

2) Operation space of cutter changing robot arm. The workspace of the robot arm determines whether it can reach the positions of all the cutter on the radial spoke. Therefore, the Monte Carlo method is used to solve the

workspace of the robot arm. According to the forward kinematics model of the robot arm, the parameters of each joint are assigned by the random function in MATLAB, and the reachable workspace of the arm can be obtained. The calculation model of joint random variables is as follows:

$$\begin{cases} \theta_i = \theta_{imin} + rand \times (\theta_{imax} - \theta_{imin}) \\ d_i = d_{imin} + rand \times (d_{imax} - d_{imin}) \end{cases}, \tag{13}$$

where: θ_{imax}, θ_{imin}, d_{imax}, d_{imin} are the variable limits of the rotation joint and the translation joint respectively, and rand

4. Path planning of cutter changing robot arm

4.1. Inverse kinematic solution model of robot arm

Inverse kinematics is used to solve the motion parameters of joint variables when the end position and pose of robot in cartesian space system is known. Newton-Raphson method has the advantages of fast convergence and self-correction, by using the method of tangent iteration of function to approach the correct solution of the equations. According to the perturbation differential of the arm coordinate system, the Jacobian matrix of each joint is constructed, which influence the motion characteristics. The joint value corresponding to the expected end posture of the arm is solved based on Newton Raphson iterative method.

Considering the influence of each joint parameters on the end posture of the arm, six joint values about six freedom degrees of the robot arm to be solved. q_i is the ith joint variable value:

$$q_i = (d_1, \theta_2, \theta_3, \theta_4, d_5, d_6). \tag{14}$$

F is a function of six joint variables:

$$F = f(d_1, \theta_2, \theta_3, \theta_4, d_5, d_6). \tag{15}$$

By calculating the derivative of generalized velocity to time, the relationship between the end linear velocity and angular velocity of the arm and the differential change of each joint value can be obtained.

$$\begin{bmatrix} v \\ w \end{bmatrix} = \frac{dF}{dt} = J(q)\frac{dq}{dt} = \begin{bmatrix} \frac{\partial f_1}{\partial q_1} & \frac{\partial f_1}{\partial q_2} & \cdots & \frac{\partial f_1}{\partial q_6} \\ \frac{\partial f_2}{\partial q_1} & \frac{\partial f_2}{\partial q_2} & \cdots & \frac{\partial f_2}{\partial q_6} \\ \vdots & \vdots & \ddots & \vdots \\ \frac{\partial f_6}{\partial q_1} & \frac{\partial f_6}{\partial q_2} & \cdots & \frac{\partial f_6}{\partial q_6} \end{bmatrix} \cdot \frac{1}{dt} \cdot \begin{bmatrix} dq_1 \\ dq_2 \\ \cdots \\ dq_6 \end{bmatrix}. \tag{16}$$

The kinematic relationship between the linear displacement and angular displacement of the arm end and the change of each joint value is established. For the influence of the joint value change on the end coordinates of the robot arm, Eq. (16) can also be written as follows:

$$D = Jdq, \tag{17}$$

$$dq = J^{-1}D. \tag{18}$$

Because the Jacobian matrix is derived from the derivation of the corresponding kinematic equation, it is

represents random numbers from 0 to 1.

30000 groups of different random joint variables are set to represent different end positions of the robot arm in the coordinate system in the form of scattered points, and the results are shown in Fig. 10a. Fig. 10b –d respectively show the projection of end positions on the three planes of the base coordinate system XOY, YOZ and XOZ. The movement range of the arm is -2.9 m to +3.6 m in the X direction, -3.3 m to +3.3 m in the Y direction, and -0.2 m to +4.6 m in the Z direction. It indicates that the cutter change robot arm can meet the workspace requirements of the shield machine with 10 m diameter.

more complex to directly solve the Jacobian Matrix J in the relative base coordinate system. By constructing Jacobian matrix, the influence of joint motion on the pose of arm end is obtained. Firstly, the transfer matrix from the joint to be solved to the arm end is constructed as follows.

$$\begin{cases} {}^1_6T = T_2 T_3 T_4 T_5 T_6 \\ {}^2_6T = T_3 T_4 T_5 T_6 \\ {}^3_6T = T_4 T_5 T_6 \\ {}^4_6T = T_5 T_6 \\ {}^5_6T = T_6 \\ {}^6_6T = I_{4\times4} \end{cases}. \tag{19}$$

For translation joint 1 and joint 5, the differential relationship between them can be obtained.

$$\begin{bmatrix} d_x^n \\ d_y^n \\ d_z^n \\ \delta_x^n \\ \delta_y^n \\ \delta_z^n \end{bmatrix} = \begin{bmatrix} n_z \\ o_z \\ a_z \\ 0 \\ 0 \\ 0 \end{bmatrix} dd_i, \tag{20}$$

$$\begin{bmatrix} d_x^n \\ d_y^n \\ d_z^n \\ \delta_x^n \\ \delta_y^n \\ \delta_z^n \end{bmatrix} = \begin{bmatrix} (p \times n)_z \\ (p \times o)_z \\ (p \times a)_z \\ n_z \\ o_z \\ a_z \end{bmatrix} d\theta_i. \tag{21}$$

For rotation joint 1 and joint 5, the differential relationship between them can be obtained.

The transformation matrix J_i is the relationship between the joint variable and the position and pose of the arm end in Cartesian coordinate system.

$$J = \begin{bmatrix} J_1 & J_2 & J_3 & J_4 & J_5 & J_6 \end{bmatrix}. \tag{22}$$

After obtaining the Jacobian matrix of the robot arm, Newton-Raphson iterative method is used to solve the inverse solution of the arm. The steps are as follows:

1) Give initial values $q_c = (807, pi, -pi/2, -pi/2, 1310, -pi/2, 0)$, give the iterative convergence conditions $e = 0.001$.

2) Set the desired pose of arm end at the Cartesian coordinate system as T_e, and the differential motion matrix of the current arm is obtained as $\Delta = T_c^{-1} T_e - I$. According to the formula, the differential motion vector of the robot arm is obtained.

3) Substitute values of each joint into the corresponding differential Jacobian transfer matrix and establish the iterative relationship.

4) The pseudo inverse solution of the differential Jacobian transfer matrix $J+$ is obtained by SVD decomposition, and the current joint offset value is obtained by.

5) Judge whether the offset value is less than the given error $\|dq\| = \le e$. If the condition is satisfied, the iteration is exited, and the value is output. If the condition is not met, return to step 2 and repeat steps 2-5.

4.2. Cutter-changing path of robot arm

When the robot arm carries out the cutter change, it is necessary to plan the trajectory. Firstly, the position and pose of each path point which the cutter centroid passes through is transformed by the inverse kinematics of the arm, and the joint variable values are obtained. Then, through interpolation calculation, the joint variable value is expressed as a function of time, so that the end of the arm passes through the starting point and each path in the middle, and finally reaches the end point.
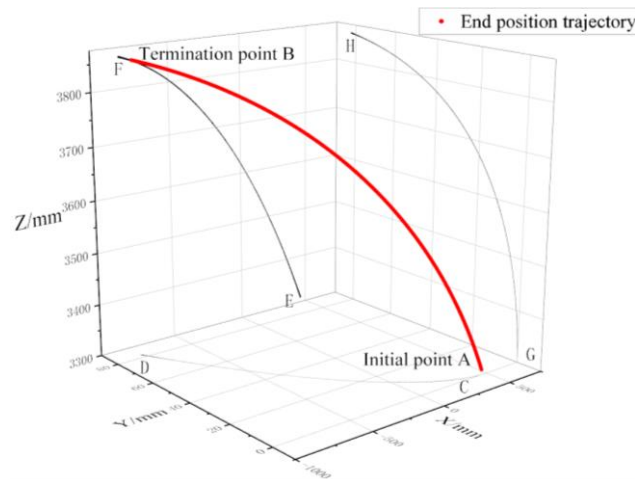

Fig. 11 Change track of centroid position of cutter

Table 2

Posture of robot arm for different cutters

Cutter number	d_1/mm	θ_2/°	θ_3/°	θ_4/°	d_5/mm	θ_6/°
25	2068	97.81	15.11	11.08	1790	-26.19
26	2064	97.81	15.04	8.98	1763	-24.03
27	2018	97.81	11.66	10.84	1781	-22.5
28	2052	97.81	13.36	6.46	1719	-19.82
29	1990	97.81	12.06	5.21	1754	-17.27
30	2076	97.81	6.52	11.47	1659	-18
31	1913	97.81	11.89	-0.07	1790	-11.83

The quintic polynomial interpolation is used to plan the trajectory of the cutter change robot. Set the initial variables of each joint as q_c = (807 mm, 180°, -90°, -90°, 1310 mm, -90°). The centroid coordinate of the end cutter is (460, 0, 3309), and the target position is (-820, 82, 3857).

The joint variable of the termination point is obtained by inverse kinematics as q_e = (1067.7 mm, 176.6°, -81°, -66.9°, 1924 mm, -103.5°). At the target position, the motion trajectory of cutter centroid in three-dimensional space is shown as Fig. 11. A is the starting point of arm, and B is the ending point. The curves CD, EF and GH are the projections of the trajectory on the XY, XZ and YZ planes respectively.

Similarly, the posture planning of the robot arm can be obtained, taking 7 cutters on a spoke as the target position, respectively, as shown in Table 2.

5. Verification of cutter changing robot arm

5.1. Dynamic analysis of cutter changing robot arm

Collecting the time-displacement relationship of each joint, the centroid motion parameters of cutter can be obtained. The centroid velocity and acceleration of cutter in X, Y and Z directions are shown in Fig. 12, respectively. It can be seen that the velocity and acceleration in X, Y and Z axes are relatively stable and smooth, and there are no discontinuities and mutation points in the whole movement process.
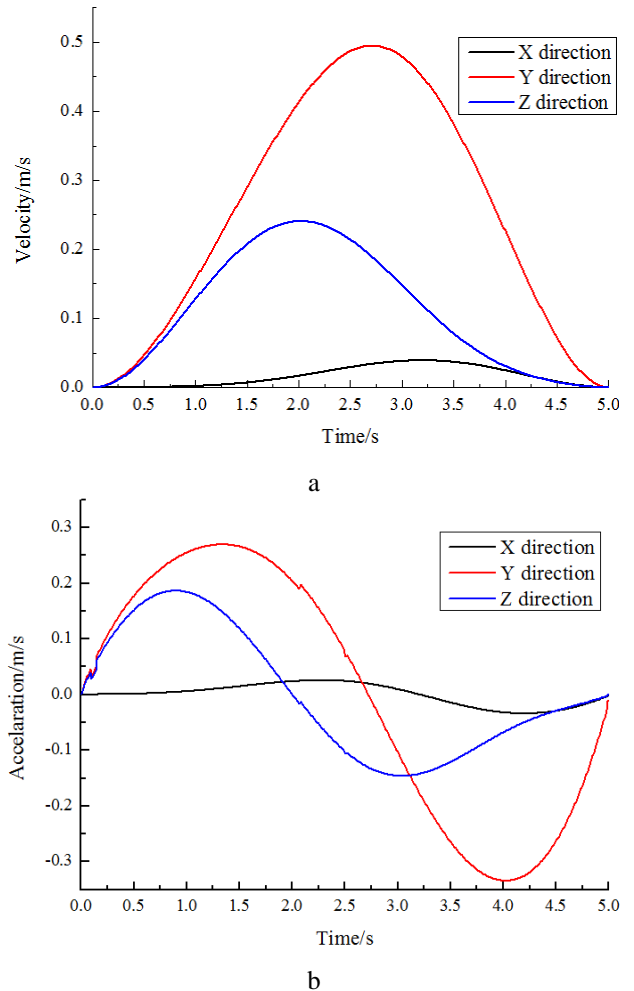

a

b

Fig. 12 Centroid velocity and acceleration of cutter: a) centroid velocity of cutter; b) centroid acceleration of cutter

Joints 1, 3, 4, 5 of the arm are driven by the hydraulic cylinder, and the displacement-time relationship of three hydraulic cylinders can be obtained, as shown in Fig. 13, a. In addition, driving torque curve of hydraulic cylinder and

swing cylinder is obtained as Fig. 13, b. It varies in the normal range, and the whole movement process is smooth, the power output is stable. It indicates that each joint of the robot arm performs stably without obvious impact and vibration in the actual process of cutter change.
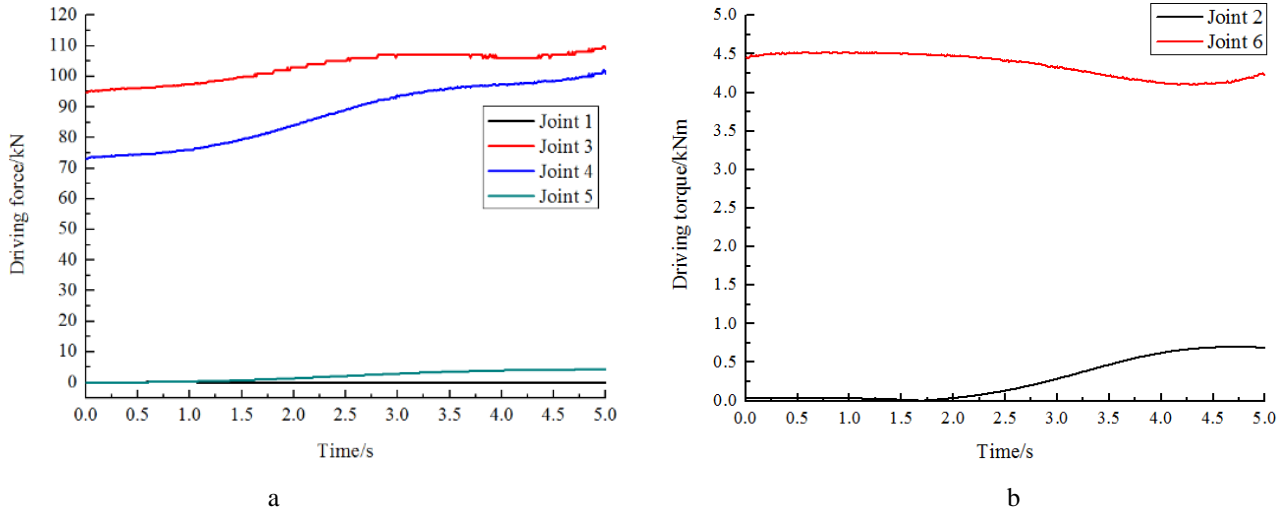

a

b

Fig. 13 Curve of hydraulic cylinder drive force and torque: a) curve of hydraulic cylinder drive force; b) curve of hydraulic cylinder drive torque

5.2. Test bench of cutter changing robot arm

A prototype of cutter changing robot is made to verify the motion characteristics of the robot arm, as Fig. 14 shown. The cutter to be replaced is placed in cutter housing with different installation radius to simulate cutterhead. Cutter-changing operations at different location with different motion path are carried out, where the posture of the robot arm is monitored real time. The experimental results show that the designed cutter change robot can reach different cutter positions.
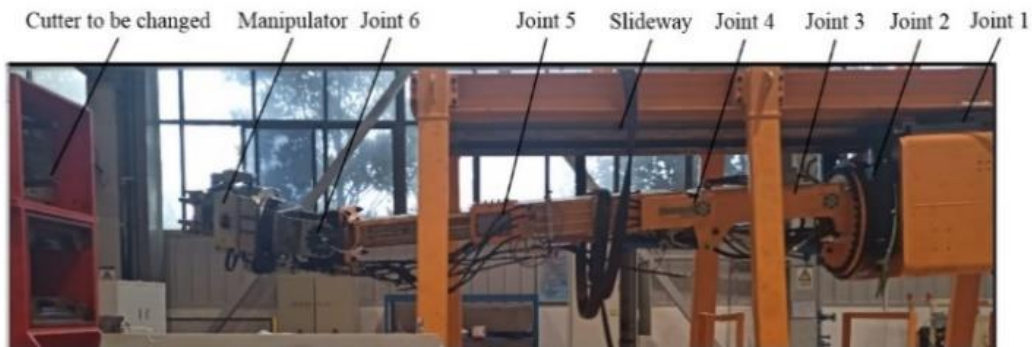

Fig. 14 Test bench of cutter changing robot

6. Conclusions

The inner space structure characteristics of the shield machine was analyzed and the robot installation position and the distribution area of cutter to be replaced were determined. A design scheme of 4R2T 6-DOF cutter change robot arm suitable for shield machine was proposed. The optimization objective is to minimize the workspace and the total length of the connecting rod, and the structural dimension parameters of the manipulator are designed. Taking the minimum working space and total length of the connecting rod as optimization target, the design of the structural dimension parameters of the robot arm is completed.

Based on the joint characteristics of the robot arm, D-H method was used to establish the kinematic coordinate system, and its MD-H parameters were defined. The workspace of the robot was analyzed by Monte Carlo method. The results show that the robot arm can meet the needs of the shield machine with a diameter of less than 10 m.

The Jacobian matrix of the robot arm was established, and the Newton Raphson iterative method was used to solve the inverse kinematics. The position and pose of each joint of the robot arm for different target cutters were obtained, and the trajectory planning of the robot arm replacement operations for all cutters on the radial arm was completed. The feasibility of the robot arm was verified through the cutter change operation posture and the movement performance test.

References

1. **Küpferle, J.; Zizka, Z.; Schoesser, B.; Röttger, A.; Alber, M.; Thewes, M.; Theisen, W.** 2018. Influence of the slurry-stabilized tunnel face on shield TBM tool wear regarding the soil mechanical changes–Experimental evidence of changes in the tribological system, Tunnelling and Underground Space Technology 74: 206-216.
http://dx.doi.org/10.1016/j.tust.2018.01.011.

2. **Li, X.; Gong, G.** 2019. Predictive control of slurry pressure balance in shield tunneling using diagonal recurrent neural network and evolved particle swarm optimization, Automation in Construction 107: 102928.
http://dx.doi.org/10.1016/j.autcon.2019.102928.

3. **Huo, J.; Wang, W.; Sun, W.; Ling, J.; Dong, J.** 2017. The multi-stage rock fragmentation load prediction model of tunnel boring machine cutter group based on dense core theory, The International Journal of Advanced Manufacturing Technology 90 (1-4): 277-289.
http://dx.doi.org/10.1007/s00170-016-9375-9.

4. **Balta, G.; Dikmen, I.; Birgonul, M.** 2021. Bayesian network based decision support for predicting and mitigating delay risk in TBM tunnel projects, Automation in Construction 129: 103819.
http://dx.doi.org/10.1016/j.autcon.2021.103819.

5. **Li, Y.; Di, H.; Yao, Q.; Fu, L.; Zhou, S.** 2020. Prediction model for disc cutter wear of tunnel boring machines in sandy cobble strata, KSCE Journal of Civil Engineering 24 (3): 1010-1019.
http://dx.doi.org/10.1007/s12205-020-1631-8.

6. **Fang, Y.; Yao, Z.; Xu, W.; Tian, Q.; He, C.; Liu, S.** 2021. The performance of TBM disc cutter in soft strata: A numerical simulation using the three-dimensional RBD-DEM coupled method, Engineering Failure Analysis 119: 104996.
http://dx.doi.org/10.1016/j.engfailanal.2020.104996.

7. **Sun, H.; Guo, W.; Liu, J.; Song, L.; Liu, X.** 2018. Layout design for disc cutters based on analysis of TBM cutter-head structure, Journal of Central South University 25 (4): 812-830.
http://dx.doi.org/10.1007/s11771-018-3786-8.

8. **Dai, W.; Xia, Y.; Xu, H.; Yang, M.** 2020. Numerical simulation of freezing effect and tool change of shield machine with a frozen cutterhead, Journal of Central South University 27 (4): 1262-1272.
http://dx.doi.org/10.1007/s11771-020-4365-3.

9. **Han, M.; Cai, Z.; Qu, C.** 2019. On the loads for strength design of cutterhead of full face rock tunnel boring machine, Chinese Journal of Mechanical Engineering 32 (1): 1-12.
http://dx.doi.org/10.1186/s10033-019-0411-.1

10. **Farrokh, E.** 2021. Cutter change time and cutter consumption for rock TBMs, Tunnelling and Underground Space Technology 114: 104000.
http://dx.doi.org/10.1016/j.tust.2021.104000.

11. **Bogue, R.** 2014. Snake robots: a review of research, products and applications, Industrial Robot 41 (3): 253.
http://dx.doi.org/10.1108/IR-02-2014-0309.

12. **NeTTun.** 2017. New technologies for tunnelling and underground works [online], Available from Internet: http://robotik.dfki-bremen.de/en/research/projects/nettun.html.

13. **Meng, Z.; Yang, D.; Huo, J.; Zhao, P.; Bao, Y.** 2021. Development and performance evaluation of an integrated disc cutter system for TBMs, Applied Sciences 11 (2): 644.
http://dx.doi.org/10.3390/app11020644.

14. **Xia, Y.; Yang, M.; Ji, Z.; Jia, L.; Zhou, Z.; Wu, D.** 2021. Design and dimension optimization of cutter disassembly mechanism for shield tunneling machine, Journal of Mechanical Science and Technology 35 (7): 3005-3018.
http://dx.doi.org/10.1007/s12206-021-0624-y.

15. **Yang, D.; Meng, Z.; Guo, Z.; Huo, J.** 2021. Trajectory planning of TBM cutter changing robot based on binocular vision, IEEE Asia-Pacific Conference on Image Processing, Electronics and Computers (IPEC), 2021: 1318-1322.
http://dx.doi.org/10.1109/ipec51340.2021.9421344.

16. **Gao, G.; Sun, G.; Na, J.; Guo, Y.; Wu, X.** 2018. Structural parameter identification for 6 DOF industrial robots, Mechanical Systems and Signal Processing 113: 145-155.
http://dx.doi.org/10.1016/j.ymssp.2017.08.011.

17. **Li, J.; Yu, H.; Shen, N.; Zhong, Z.; Lu, Y.; Fan, J.** 2021. A novel inverse kinematics method for 6-DOF robots with non-spherical wrist, Mechanism and Machine Theory 157: 104180.
http://dx.doi.org/10.1016/j.mechmachtheory.2020.104180.

18. **Ye, H.; Wang, D.; Wu, J.; Yue, Y.; Zhou, Y.** 2020. Forward and inverse kinematics of a 5-DOF hybrid robot for composite material machining, Robotics and Computer-Integrated Manufacturing 65: 101961.
http://dx.doi.org/10.1016/j.rcim.2020.101961.

19. **Xie, B.; Qin, M.; Song, D.; Wu, D.** 2020. Design of automatic tunnel shotcrete robotic system for 8-DOF, Journal of Huazhong University of Science And Technology (Natural Science Edition) 48 (1): 115-120. (in Chinese).
http://dx.doi.org/10.13245/j.hust.200121.

20. **Wang, Y.; Zhao, C.; Wang, X.; Zhang, P.; Li, P.; Liu, H.** 2021. Inverse kinematics of a 7-DOF spraying robot with 4R 3-DOF non-spherical wrist, Journal of Intelligent & Robotic Systems 101 (4): 1-17.
http://dx.doi.org/10.1007/s10846-021-01338-w.

21. **Zhang, Z.; Yang, Q.; Zhao, J.; Chang, B.; Liu, X.** 2020. Kinematic synthesis method for the one-degree-of-freedom jumping leg mechanism of a locust-inspired robot, Science China Technological Sciences 63 (3): 472-487.
http://dx.doi.org/10.1007/s11431-019-9750-6.

22. **Liu, Y.; Yu, C.; Sheng, J.; Zhang, T.** 2018. Self-collision avoidance trajectory planning and robust control of a dual-arm space robot, International Journal of Control, Automation and Systems 16 (6): 2896-2905.
http://dx.doi.org/10.1007/s12555-017-0757-z.

23. **Zhang, J.; Meng, Q.; Feng, X.; Shen, H.** 2018. A 6-DOF robot-time optimal trajectory planning based on an improved genetic algorithm, Robotics and Biomimetics 5 (1): 1-7.
http://dx.doi.org/10.1186/s40638-018-0085-7.

24. **Fung, R.; Cheng, Y.** 2014. Trajectory planning based on minimum absolute input energy for an LCD glass-

handling robot, Applied Mathematical Modelling 38 (11-12): 2837-2847.

http://dx.doi.org/10.1016/j.apm.2013.11.017.

25. **Li, T.; Sun, K.; Xie, Z. W.; Liu, H.** 2011. Optimal measurement configurations for kinematic calibration of six-DOF serial robot, Journal of Central South University 18 (3): 618-626.

http://dx.doi.org/10.1007/s11771-011-0739-x.

26. **Xu, W.; Yan, L.; Hu, Z.; Liang, B.** 2019. Area-oriented coordinated trajectory planning of dual-arm space robot for capturing a tumbling target, Chinese Journal of Aeronautics 32 (9): 2151-2163.

http://dx.doi.org/10.1016/j.cja.2019.03.018.

27. **Augustaitis, A; Jurenas, V; Kulvietis, G.** 2018 Kinematics of trunk-like robots with piezo actuators, Mechanika 24(2): 254-259.

http://dx.doi.org/10.5755/j01.mech.24.2.19205.

28. **Gong, H.; Xie, H.; Yang, H.** 2019. A numerical method for extrication characteristics of TBM cutterhead with the HVC, Chinese Journal of Mechanical Engineering 32 (1): 1-9.

http://dx.doi.org/10.1186/s10033-019-0413-z.

29. **Yang, J.; Zhang, X.; Ji, P.; Liu, Q.; Lu, X.; Wei, J.; Qi, S.; Fang, H.; Fang, J.; Geng, Y.** 2019. Analysis of disc cutter damage and consumption of TBM1 section on water conveyance tunnel at Lanzhou water source construction engineering, Tunnelling and Underground Space Technology 85: 67-75.

http://dx.doi.org/10.1016/j.tust.2018.11.040.

30. **Huo, J.; Xu, Z.; Meng, Z.; Li, J.; Dong, J.; Wang, L.** 2020. Coupled modeling and dynamic characteristics of TBM cutterhead system under uncertain factors, Mechanical Systems and Signal Processing 140: 106664.

http://dx.doi.org/10.1016/j.ymssp.2020.106664.

M. Yang, G. Zeng, Y. Ren, L. Lin, W. Ke, Y. Liu

ACCESSIBILITY AND TRAJECTORY PLANNING OF CUTTER CHANGING ROBOT ARM FOR LARGE-DIAMETER SLURRY SHIELD

S u m m a r y

Aiming at solving the problems of huge cost, long cycle and high risky during manual cutter changing process for shield machine, a cutter changing robot was designed to adapt to its narrow and complex space, the workspace and motion path of cutter changing robot arm were studied. Firstly, by analyzing the internal space and cutter layout characteristic, the configuration of the robot arm was proposed, and the dimension of each rod was designed using multi-objective optimization method. The kinematic model of the robot arm was established by using the D-H model method to analyze its reachable working space. While the inverse kinematic model of the robot arm was solved by the Newton-Raphson iterative method to complete the trajectory planning of the arm for all cutter locations, where the relationship between the target position and the joint variables was established. The motion stability of the robot was verified by virtual simulation and test. The results show that the working space of the designed robot arm meets the cutter changing requirements that all the cutter position can be reached. Moreover, the power output of the drive is smooth, which can transport the cutter weighing up to 250 kg.

Keywords: shield machine, cutter change robot, kinematics analysis, trajectory planning, workspace.